PHYSICAL REVIEW D **88,** 123514 (2013)

Parametrized modified gravity constraints after Planck

Bin Hu,[1] Michele Liguori,[1,2] Nicola Bartolo,[1,2] and Sabino Matarrese[1,2]

[1]*INFN, Sezione di Padova, via Marzolo 8, 35131 Padova, Italy*

[2]*Dipartimento di Fisica e Astronomia "G. Galilei", Università degli Studi di Padova, via Marzolo 8, 35131 Padova, Italy*

(Received 5 August 2013; published 9 December 2013)

We constrain $f(R)$ and chameleon-type modified gravity in the framework of the Berstchinger-Zukin parametrization using the recently released Planck data, including both the cosmic mircowave background radiation (CMB) temperature power spectrum and the lensing potential power spectrum. Some other external data sets are included, such as baryon acoustic oscillation (BAO) measurements from the 6dFGS, SDSS DR7 and BOSS DR9 surveys; Hubble Space Telescope (HST) H_0 measurements, and supernovae from the Union2.1 compilation. We also use WMAP9 data for a consistency check and comparison. For $f(R)$ gravity, WMAP9 results can only give a quite loose constraint on the modified gravity parameter B_0, which is related to the present value of the Compton wavelength of the extra scalar degree of freedom, $B_0 < 3.37$ at 95% C.L. We demonstrate that this constraint mainly comes from the late integrated Sachs-Wolfe effect. With only Planck CMB temperature power-spectrum data, we can improve the WMAP9 result by a factor 3.7 ($B_0 < 0.91$ at 95% C.L.). If the Planck lensing potential power-spectrum data are also taken into account, the constraint can be further strengthened by a factor 5.1 ($B_0 < 0.18$ at 95% C.L.). This major improvement mainly comes from the small-scale lensing signal. Furthermore, BAO, HST and supernovae data could slightly improve the B_0 bound ($B_0 < 0.12$ at 95% C.L.). For the chameleon-type model, we find that the data set that we used cannot constrain the Compton wavelength B_0 or the potential index s of the chameleon field, but it can give a tight constraint on the parameter $\beta_1 = 1.043^{+0.163}_{-0.104}$ at 95% C.L. ($\beta_1 = 1$ in general relativity), which accounts for the nonminimal coupling between the chameleon field and the matter component. In addition, we find that both modified gravity models we consider favor a relatively higher Hubble parameter than the concordance ΛCDM model in general relativity.

DOI: 10.1103/PhysRevD.88.123514 PACS numbers: 98.80.−k, 04.50.Kd, 98.80.Es

I. INTRODUCTION

Cosmic acceleration can arise from either an exotic form of energy with negative pressure, referred to as "dark energy," or a modification of gravity manifesting on large scales. As shown in [1–3], at the background level dark energy and modified gravity models are almost indistinguishable; hence, one needs to investigate the perturbation dynamics. The studies of perturbation theory in modified gravity models, in principle, can be classified into two different frameworks: the parametrization approach and the nonparametrization method, such as the principal component analysis [4–6]. In this paper we focus on the former. There exist several phenomenological- and theory-oriented parametrizations of modified gravity, such as the Bertschinger-Zukin [7] and the Brax-Davis-Li-Winther [8] parametrizations. These parametrizations are mainly suitable for the quasistatic regime, where the time evolution of the gravitational potentials is negligible compared with their spatial gradient. Furthermore, if we focus on the linear fluctuation dynamics, for which the equations in Fourier space can be reduced to simple algebraic relations, these techniques allow us to perform some analytic calculations which make the parametrization technically efficient. However, if we want to go beyond the quasistatic regime, while remaining in the linear perturbation framework, the parametrization of modified gravity becomes more complex. This is because on the largest scales, especially the superhorizon and near-horizon scales, the time evolution of the gravitational potentials is no longer negligible; the time derivative terms dominate the dynamical equations, which means that we need to solve some temporal ordinary differential equations. Actually, there exists some debate about the range of validity of the various parametrizations. For example, on one hand, as shown in [9], using a parametrization with insufficient freedom significantly tightens the apparent theoretical constraints. On the other hand, for some specific modified gravity models some phenomenological parametrizations work quite well; for instance, the authors of [10] recently demonstrated that for the small Compton wavelength case in the $f(R)$ model, the Bertschinger-Zukin parametrization [7] is practically good enough for the current data analysis purpose. This is because, on scales larger than the Compton wavelength, the deviation from general relativity is suppressed. Below the Compton scale the gravitational potential growth is enhanced and the two metric potentials are no longer equal. Consequently, for the small Compton wavelength case, whose value is less than the current horizon size, the most significant modifications with respect to general relativity occur in the subhorizon regime. In addition to the above explicit parametrizations, some

quite generic frameworks to study different modified gravity scenarios have also been proposed, such as the parametrized post-Friedmann (PPF) formalism, including the Hu-Sawicki approach [11,12], its calibration version [13] and Baker-Ferreira-Skordis-Zuntz algorithm [14,15], and effective field theory (EFT) approaches [16–23].

From the observational point of view, many windows have been proposed to constrain modified gravity models, such as the integrated Sachs-Wolfe (ISW) effect [24] in cosmic microwave background (CMB) anisotropies, including the CMB power spectrum [5,25–29], the CMB ISW-lensing bispectrum [30,31], baryon acoustic oscillation (BAO) measurements [29,32,33], the galaxy-ISW cross correlation [29,34–36], cluster abundance [37–40], peculiar velocity [41,42], redshift-space distortions [43,44], weak lensing [5,27,29,35,42,45–52], 21 cm lines [53,54], the matter power spectrum and the bispectrum [55–58]. In addition, recently some N-body simulation algorithms in modified gravity models have been developed [59–61]. As shown in [36,38,56], with WMAP resolution the modification effects on the CMB mainly come from the ISW effect, which becomes prominent on the largest scales. However, due to the unavoidable cosmic variance on large scales, the constraints from these effects are not significant. On the other hand, since the typical modification scales are in the subhorizon regime, several studies show that the most stringent constraints come from the large-scale structure data sets. For example, the strongest current constraint on $f(R)$ gravity ($B_0 < 1.1 \times 10^{-3}$, 95% C.L.) [38] is obtained through cluster abundance data sets. Various previous results show that the main constraint on modified gravity comes from galaxy or cluster scales, which corresponds to the multipole range $l \gtrsim 500$ in CMB data, where the lensing effect is no longer negligible. The recent release of Planck data [62] provides us with a fruitful late-time information both on the ISW and the lensing scales, which is encoded in the CMB temperature power spectrum [63] and lensing potential power spectrum [64], as well as the CMB temperature ISW-lensing bispectrum [65,66]. The full sky lensing potential map was first measured, and the significance of the amplitude of the lensing potential power spectrum arrives at the 25σ level. The ISW-lensing bispectrum was also first detected with nearly 3σ significance. Furthermore, through the lensing potential reconstruction and the ISW-lensing bispectrum, the ISW effect was also first detected via the CMB itself. All in all, with its high resolution the Planck mission provides us with fruitful information about the Universe's late-time acceleration. For example, the authors of [67] show that the joint analysis of Planck and BAO data could greatly improve the Brans-Dicke parameter ω constraint. Further new constraint results related with modified gravity or dark energy can be found in [68–72].

Due to these considerations, in this paper we investigate the power of the Planck data sets in constraining modified gravity scenarios. In order to break the parameter degeneracies, apart from Planck data sets, we also use some external astrophysical data sets, such as BAO measurements from the 6dFGS, SDSS DR7 and BOSS DR9 surveys; H_0 from Hubble Space Telescope (HST) measurements; and supernovae from the Union2.1 compilation. We also use WMAP9 data for a consistency check and comparison. Because of the simplicity of the Bertschinger-Zukin parametrization, in this paper we study the modified gravity theory through this method.

II. BERTSCHINGER-ZUKIN PARAMETRIZATION

As pointed out in [8], a large class of modified gravity theories, e.g., chameleon [73,74], symmetron [75–77] and dilaton [78] models, can be characterized by the mass of a suitable scalar field and the coupling between the scalar field and baryonic or dark matter components. In the Einstein frame, where the gravitational sector is the standard Einstein-Hilbert action, the scalar field is exponentially coupled with the matter sector,

$$S_{\rm E} = \int {\rm d}^4x\sqrt{-\tilde{g}}\left[\frac{M_{\rm pl}^2}{2}\tilde{R} - \frac{1}{2}\tilde{g}^{\mu\nu}(\tilde{\nabla}_\mu\phi)(\tilde{\nabla}_\nu\phi) - V(\phi)\right] + S_i(\chi_i, e^{-\kappa\alpha_i(\phi)\tilde{g}_{\mu\nu}}), \quad (1)$$

where the Einstein frame metric $\tilde{g}_{\mu\nu}$ is related to the Jordan frame metric $g_{\mu\nu}$ through a conformal transformation

$$\tilde{g}_{\mu\nu} = e^{\kappa\alpha_i(\phi)}g_{\mu\nu}, \quad (2)$$

and χ_i denotes the matter components.

Inspired by some nice properties in the quasistatic regime of the $f(R)$ model, Bertschinger and Zukin in [7] first wrote the two gravitational potentials in the conformal Newtonian gauge[1] in terms of two observation-related variables, the time- and scale-dependent Newton constant $G\mu(a, k)$ and the so-called gravitational slip $\gamma(a, k)$,

$$k^2\Psi = -4\pi G a^2\mu(a, k)\rho\Delta, \quad (3)$$

$$\frac{\Phi}{\Psi} = \gamma(a, k), \quad (4)$$

where G is the Newton constant in the laboratory. The corresponding Einstein-Boltzmann solver named MGCAMB is implemented in [49,79]. In this paper, we implement the same algorithm in the new version of CAMB [80], which is compatible with the Planck likelihood.

In the following sections, we will study $f(R)$ gravity and the quite general chameleon-type model in the framework of the Bertschinger-Zukin parametrized modified gravity method, by using the Planck [63,64], WMAP9 [81,82] and some external astrophysical data.

[1]We take the convention that ${\rm d}s^2 = -(1 + 2\Psi){\rm d}t^2 + a^2(1 - 2\Phi){\rm d}x^2$.

TABLE I. List of the parameters used in the Monte Carlo sampling.

Parameter	Range (min, max)
$\Omega_b h^2$	(0.005, 0.100)
$\Omega_c h^2$	(0.01, 0.99)
$100\vartheta_*$	(0.5, 10.0)
τ	(0.01, 0.80)
n_s	(0.5, 1.5)
$\ln(10^{10}A_s^2)$	(2.7, 4.0)

MG parameters	$f(R)$	Chameleon
B_0	(0, 10)	(0, 1)
β_1	4/3	(0.001, 2)
s	4	(1, 4)

A. $f(R)$ model

Due to the simplicity of its Lagrangian, $f(R)$ gravity has received much attention (see the recent review [83] and references therein), especially as an illustration of the chameleon mechanism. Besides the simplicity of the structure of this theory, there are two more reasons for the interest it attracted. One is that the form of the function $f(R)$ can be engineered to exactly mimic *any* background history via a one-parameter family of solutions [2]. The second reason is that $f(R)$ gravity gives a slightly better fit than at ΛCDM, which can be attributed to the lowering of the temperature anisotropy power spectrum in the small l regime [38]. In this paper we consider the class of $f(R)$ gravity models which can mimic a ΛCDM background.

Because of the higher order derivative nature of $f(R)$ gravity, there exists a scalar degree of freedom, named the scalaron, $f_R \equiv \mathrm{d}f/\mathrm{d}R$, with mass

$$m_{f_R}^2 \equiv \frac{\partial^2 V_{\mathrm{eff}}}{\partial f_R^2} = \frac{1}{3}\left(\frac{1+f_R}{f_{RR}} - R\right). \tag{5}$$

Then the Compton wavelength of the scalaron reads

$$\lambda_{f_R} \equiv m_{f_R}^{-1}. \tag{6}$$

Usually, it is convenient to use the dimensionless Compton wavelength

$$B \equiv \frac{f_{RR}}{1+f_R} R' \frac{H}{H'}, \tag{7}$$

with $f_{RR} = \mathrm{d}^2 f/\mathrm{d}R^2$ and $' = \mathrm{d}/\mathrm{d}\ln a$.

In the Bertschinger-Zukin parametrization [7], the explicit expressions of the functions $\mu(a,k)$ and $\gamma(a,k)$ for $f(R)$ gravity read

$$\mu(a,k) = \frac{1+\frac{4}{3}\lambda_1^2 k^2 a^4}{1+\lambda_1^2 k^2 a^4}, \tag{8}$$

TABLE II. Best-fit values and 68% confidence limits for $f(R)$ gravity (and 95% confidence limits in parentheses for B_0). The first column shows the consistency check of the code in the general relativity limit.

	GR limit: Planck + WP		BZ: WMAP9		Planck + WP		+lensing		+BAO + HST + Union2.1	
Parameters	Best fit	68% limit	Best fit	68% limit	Best fit	68% limit	Best fit	68% limit	Best fit	68% limit
$\Omega_b h^2$	0.02266	0.02206 ± 0.00028	0.02270	0.02271 ± 0.00052	0.02250	0.02253 ± 0.00031	0.02227	0.02247 ± 0.00031	0.02232	0.02244 ± 0.00026
$\Omega_c h^2$	0.1201	0.1198 ± 0.0027	0.1147	0.1134 ± 0.0046	0.1178	0.1164 ± 0.0026	0.1173	0.1151 ± 0.0026	0.1180	0.1157 ± 0.0016
100θ	1.04151	1.04132 ± 0.00063	1.0410	1.0405 ± 0.0023	1.0420	1.04190 ± 0.00065	1.0418	1.0419 ± 0.00064	1.0413	1.0418 ± 0.00057
τ	0.083	0.090 ± 0.013	0.086	0.090 ± 0.014	0.077	0.087 ± 0.013	0.103	0.085 ± 0.013	0.092	0.084 ± 0.012
n_s	0.9601	0.9607 ± 0.0073	0.973	0.974 ± 0.014	0.967	0.970 ± 0.0075	0.970	0.971 ± 0.0076	0.965	0.970 ± 0.0056
$\log(10^{10}A_s)$	3.077	3.090 ± 0.025	3.092	3.093 ± 0.031	3.063	3.078 ± 0.025	3.111	3.070 ± 0.024	3.091	3.069 ± 0.024
B_0	...	...	0.015	$<1.94(3.37)$	0.121	$<0.38(0.91)$	0.023	$<0.054(0.18)$	0.0044	$<0.041(0.12)$
Ω_Λ	0.684	0.685 ± 0.016	0.715	0.719 ± 0.026	0.701	0.707 ± 0.015	0.702	0.713 ± 0.015	0.697	0.711 ± 0.0092
H_0[km/s/Mpc]	67.25	67.34 ± 1.19	69.59	69.92 ± 2.23	68.64	69.09 ± 1.24	68.56	69.54 ± 1.26	68.15	69.27 ± 0.76
$\chi^2_{\mathrm{min}}/2$	4902.724		3779.201		4900.427		4907.413		4975.704	

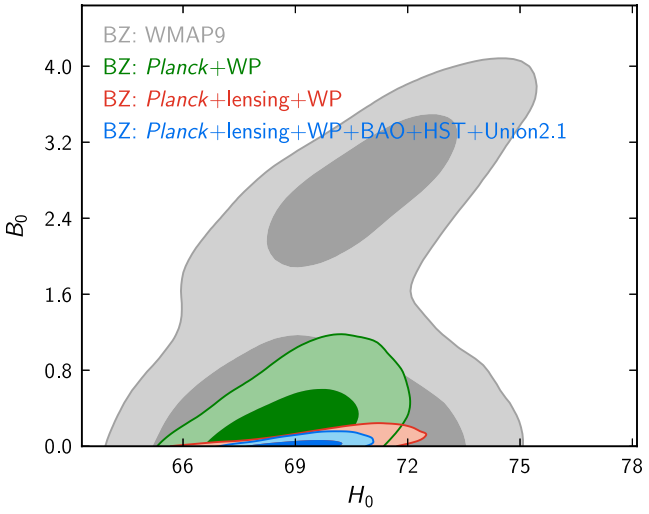

FIG. 1 (color online). Two-dimensional contour diagram of B_0 and H_0. The appearance of the upper dark gray area is due to the nonlinear dependence of the ISW effect on B_0.

$$\gamma(a,k) = \frac{1+\frac{2}{3}\lambda_1^2 k^2 a^4}{1+\frac{4}{3}\lambda_1^2 k^2 a^4}, \tag{9}$$

based on the quasistatic approximation. The above parametrization is improved by Giannantonio *et al.* in [34] to take the ISW effect into account through some empirical formula

$$\mu(a,k) = \frac{1}{1-1.4\times 10^{-8}|\lambda_1|^2 a^3}\,\frac{1+\frac{4}{3}\lambda_1^2 k^2 a^4}{1+\lambda_1^2 k^2 a^4}. \tag{10}$$

For this reason, in our numerical calculation we use (10) instead of the original expression (8).

Through a few simple computations, one can easily find that λ_1 is nothing but the present Compton wavelength

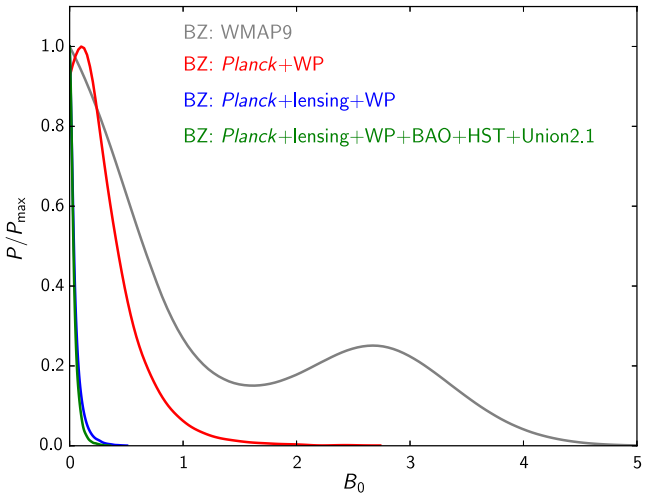

FIG. 2 (color online). The likelihood of B_0. The second peak in the gray curve is due to the nonlinear dependence of the ISW effect on B_0.

$\lambda_1^2 = B_0 c^2/(2H_0^2)$. Remember that Song *et al.* in [2] pointed out that there exists a one-parameter family solution in $f(R)$ gravity which could mimic any background evolution. Conventionally, we choose this one-parameter family labeled by the Compton wavelength at present B_0 or λ_1^2 in the Bertschinger-Zukin parametrization. Given the above analysis, we can see that in $f(R)$ gravity, compared with the concordance ΛCDM model, there is only one extra parameter, B_0, which makes the effects of gravitational modification quite manifest.

B. Chameleon-type model

The chameleon models [73,74] are characterized by a runaway potential and a nearly constant coupling α. Since the $f(R)$ model can be seen as a specific chameleon model, it is straightforward to generalize the Bertschinger-Zukin parametrization for $f(R)$ gravity (8) and (9) into

$$\mu(a,k) = \frac{1+\beta_1\lambda_1^2 k^2 a^s}{1+\lambda_1^2 k^2 a^s}, \tag{11}$$

$$\gamma(a,k) = \frac{1+\beta_2\lambda_2^2 k^2 a^4}{1+\lambda_2^2 k^2 a^4}, \tag{12}$$

where the parameters need to satisfy the following relation,

$$\beta_1 = \frac{\lambda_2^2}{\lambda_1^2} = 2-\beta_2\frac{\lambda_2^2}{\lambda_1^2}, \tag{13}$$

and $1 \le s \le 4$. Via the above constraints the number of free parameters can be reduced to 3; usually, one chooses them as (s, β_1, λ_1). In [34,79] this kind of parametrization is called a Yukawa-type model, due to the Yukawa-type interaction between dark matter particles.

Because of the nonminimal coupling, the dynamics of the scalar field is determined jointly by the scalar field and the matter component; for example, the effective potential of the scalar field is defined by

$$V_{\rm eff}(\phi) = V(\phi) + \bar{\rho}_i e^{\kappa\alpha_i(\phi)}, \tag{14}$$

which gives an effective mass of the chameleon field

$$m^2 = V''_{\rm eff} = V'' - \kappa(\alpha'' + \alpha'^2)V', \tag{15}$$

where primes denote differentiation with respect to the field. For simplicity, here we assume that the chameleon field couples to all the matter components uniformly. Following some calculations as in [49,74], we can obtain the following relations:

$$\alpha^{1+s/2} = \frac{m_0}{m}, \qquad \lambda_1^2 = \frac{1}{m_0^2}, \qquad \lambda_2^2 = \frac{1}{m_0^2}\left(1+\frac{\alpha'^2}{2}\right),$$
$$\beta_1 = 1+\frac{\alpha'^2}{2}, \qquad \beta_2 = \frac{2-\alpha'^2}{2+\alpha'^2}, \tag{16}$$

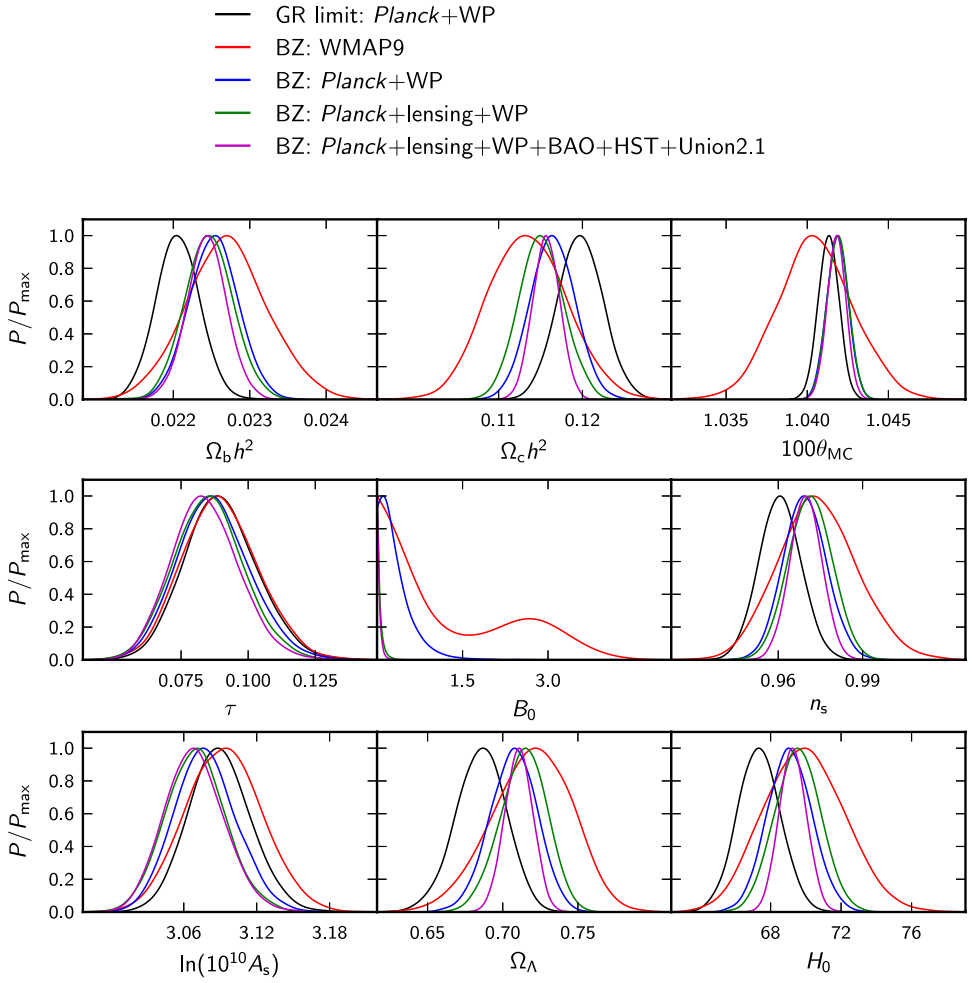

FIG. 3 (color online). Full set of parameter likelihoods in $f(R)$ gravity.

where m_0 is the chameleon effective mass at present. Furthermore, for the case of the inverse power-law potential, $V(\phi) \propto \phi^{-n}$, with $n > 0$, we have

$$n = \frac{4 - s}{s - 1}. \tag{17}$$

Here λ_1 can be replaced with the conventional parameter B_0, with the same expression in the $f(R)$ model, namely, $\lambda_1^2 = B_0 c^2/(2H_0^2)$. Through the above relations, we can easily see that the parameters β_1, B_0 and s correspond to the nonminimal coupling between the chameleon field and the matter sector, the relative Compton wavelength of the chameleon field, and the potential index of the chameleon field, respectively. Moreover, the general relativity limit corresponds to $\beta_1 = 1$, $B_0 = 0$, $s = 4$ [49].

III. DATA ANALYSIS METHODOLOGY

The purpose of this paper is to test possible deviations from general relativity on various cosmic scales by using the recent Planck data, including both the CMB temperature and lensing potential power spectra and also some external astrophysical data sets. In the following section, we will briefly review the Planck likelihood and data set which we used in this work.

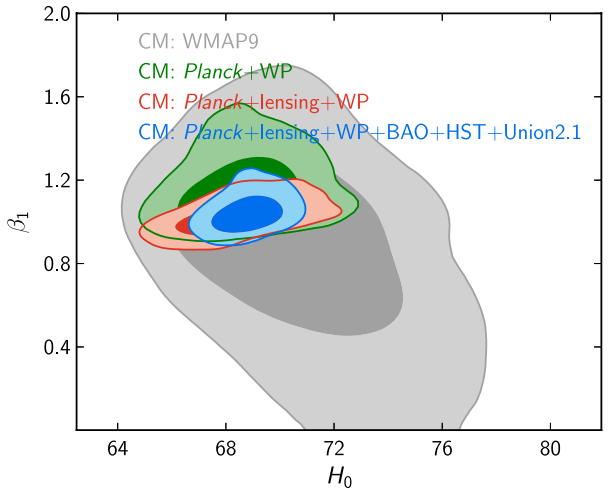

FIG. 4 (color online). Two-dimensional contour of β_1 and H_0.

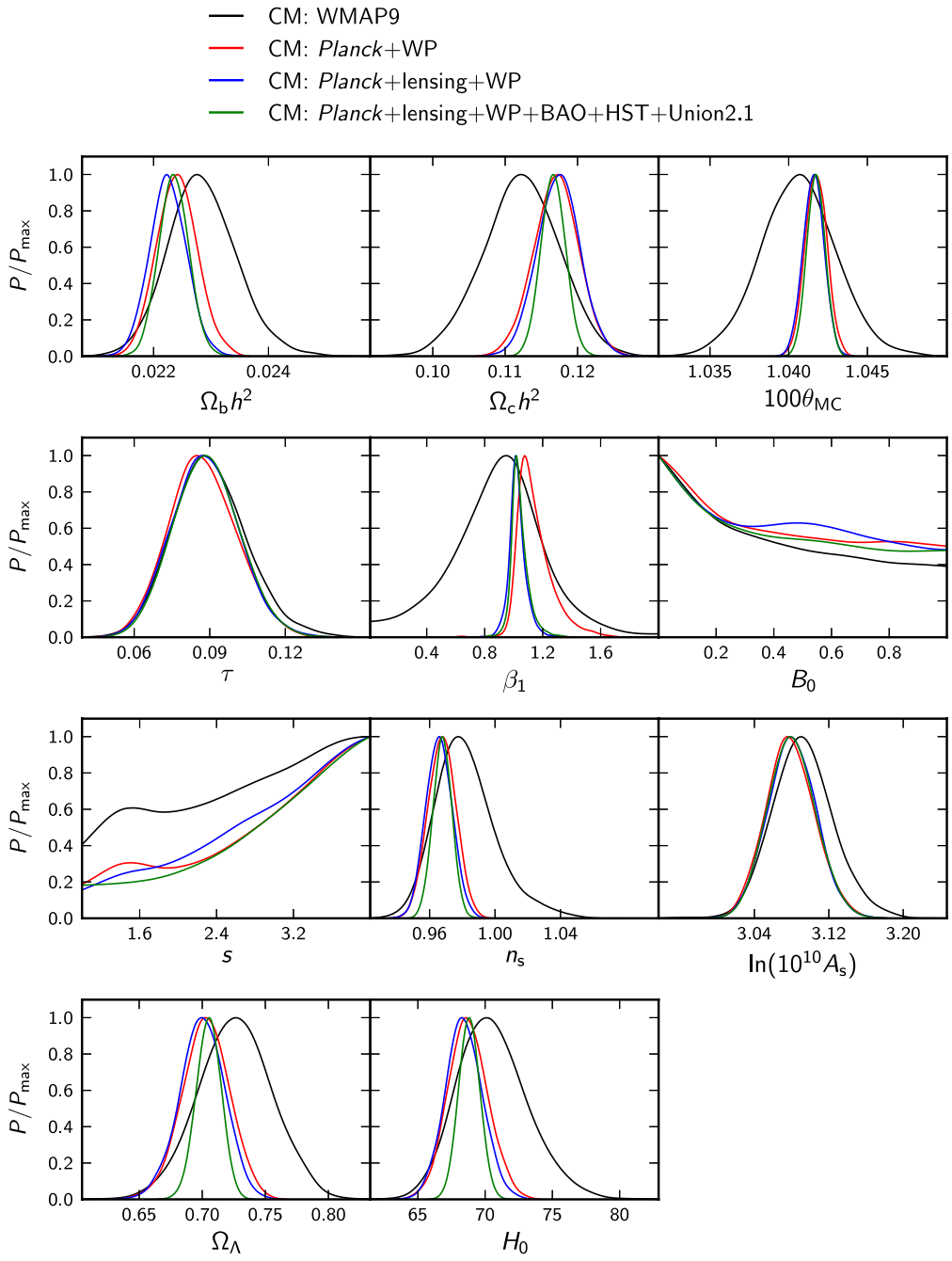

FIG. 5 (color online). Full set of parameter likelihoods in the chameleon-type model.

The total Planck CMB temperature power-spectrum likelihood is divided into low-l ($l < 50$) and high-l ($l \geq 50$) parts. This is because the central limit theorem ensures that the distribution of the CMB angular power spectrum C_l in the high-l regime can be well approximated by Gaussian statistics. However, for the low-l part the C_l distribution is non-Gaussian. For these reasons the Planck team adopts two different methodologies to build the likelihood. In detail, for the low-l part, the likelihood exploits all Planck frequency channels from 30 to 353 GHz, separating the cosmological CMB signal from diffuse Galactic foregrounds through a physically motivated Bayesian component separation technique. For the high-l part, the Planck team employed a correlated Gaussian likelihood approximation, based on a fine-grained set of angular cross spectra derived from multiple detector combinations between the 100, 143, and 217 GHz frequency channels, marginalizing over power-spectrum foreground templates. In order to break the well-known parameter degeneracy between the reionization optical depth τ and the scalar index n_s, the Planck team

TABLE III. Best-fit values and 68% confidence limits for the chameleon-type model (and 95% confidence limits in parentheses for β_1).

	CM: WMAP9		CM: Planck + WP		+lensing		+BAO + HST + Union 2.1	
Parameters	Best fit	68% limit	Best fit	68% limit	Best fit	68% limit	Best fit	68% limit
$\Omega_b h^2$	0.02279	0.02286 ± 0.00059	0.02256	0.02241 ± 0.00035	0.02226	0.02225 ± 0.00032	0.02240	0.02235 ± 0.00026
$\Omega_c h^2$	0.1184	0.1122 ± 0.0052	0.1168	0.1171 ± 0.0031	0.1162	0.1174 ± 0.0029	0.1168	0.1166 ± 0.0017
100θ	1.0391	1.0406 ± 0.0024	1.04158	1.04174 ± 0.00068	1.04183	1.04158 ± 0.00065	1.04159	1.04173 ± 0.00057
τ	0.092	0.090 ± 0.015	0.088	0.087 ± 0.013	0.089	0.088 ± 0.013	0.090	0.089 ± 0.013
n_s	0.9879	0.9825 ± 0.019	0.9686	0.9676 ± 0.0084	0.9659	0.9658 ± 0.0079	0.9698	0.9678 ± 0.0057
$\log(10^{10} A_s)$	3.131	3.092 ± 0.033	3.082	3.079 ± 0.026	3.079	3.081 ± 0.025	3.085	3.080 ± 0.025
β_1	0.954	$0.893^{+0.647}_{-0.695}$	1.127	$1.148^{+0.274}_{-0.194}$	1.033	$1.027^{+0.140}_{-0.114}$	1.020	$1.043^{+0.163}_{-0.104}$
B_0	0.496	...	0.849	...	0.473	...	0.079	...
s	1.143	...	3.398	...	3.152	...	3.635	...
Ω_Λ	0.691	0.726 ± 0.029	0.705	0.703 ± 0.018	0.701	0.700 ± 0.017	0.704	0.705 ± 0.0098
H_0 [km/s/Mpc]	67.64	70.58 ± 2.59	68.88	68.73 ± 1.46	68.93	68.43 ± 1.36	68.75	68.82 ± 0.78
$\chi^2_{\rm min}/2$		3778.939		4900.274		4907.445		4975.853

assumed the low-l WMAP polarization likelihood (WP). Apart from the CMB power spectrum, the first Planck data release provides, for the first time, a full-sky lensing potential map, by using the 100, 143, and 217 GHz frequency bands with an overall significance greater than 25σ. As we know, the lensing potential distribution follows that of the large-scale structures which form and grow mainly in the late-time universe. Thus, this map carries fruitful information about dark energy and modified gravity in this period. Hence, we expect that the lensing potential power spectrum could provide us with a stringent constraint on deviations from general relativity.

Given the above considerations, we perform our parameter estimation algorithms by using two different data sets from the Planck mission, namely, the Planck CMB power spectrum [63] and the lensing potential power spectrum [64]. In order to compare with the previous WMAP results, we also do the same analysis by using the WMAP9 data [82]. Furthermore, in order to break the parameter degeneracies we also use some other external data sets, including baryon acoustic oscillation (BAO) measurements from the 6dFGS [84], SDSS DR7 [85], and BOSS DR9 [86] surveys; Hubble Space Telescope (HST) Key Project [87] H_0 measurements; and supernovae from the Union2.1 compilation [88]. For BAO data sets, we use three redshift surveys: the 6dF Galaxy Survey measurement at $z = 0.1$, the reanalyzed SDSS-DR7 BAO measurement [89] at effective redshift $z_{\rm eff} = 0.35$, and the BOSS-DR9 measurement at $z_{\rm eff} = 0.2$ and $z_{\rm eff} = 0.35$. For the direct measurement of the Hubble constant, we use the result $H_0 = 73.8 \pm 2.4\ {\rm km\,s^{-1}\,Mpc^{-1}}$ [90], which comes from the supernova magnitude-redshift relation calibrated by the HST observations of Cepheid variables in the host galaxies of eight SNe Ia. For supernovae, we use the Union2.1 compilation, consisting of 580 SNe, calibrated by the SALT2 light-curve fitting model.

As previously stated, we implement the same algorithms of MGCAMB [49,79] in the new version of CAMB [80], which is compatible with the Planck likelihood. We sample the cosmological parameter space, which can be read in Table I, with a Markov chain Monte Carlo (MCMC) method with the publicly available code COSMOMC [91].

IV. RESULTS AND DISCUSSION

As a first step we checked the reliability of the code in the general relativity limit [$B_0 = 0$ for the $f(R)$ gravity case, $B_0 = 0$, $\beta_1 = 1$, $s = 4$ for a chameleon-type model]. We find that our results are in quite good agreement with the Planck results [92]. Here we show our consistency check for the $f(R)$ case explicitly in Table II.

The global analysis results for $f(R)$ gravity can be read in the second, third, fourth and fifth columns of Table II, which are based on WMAP9, Planck + WP, Planck + WP + lensing and Planck + WP + lensing + BAO + HST + Union 2.1 data sets.

First, we can see that the Planck CMB temperature power spectrum with WP can give an upper bound of $B_0 < 0.91$ (hereafter, we quote the significance at 95% C.L. for a modified gravity parameter, such as B_0 and β_1). Compared with the WMAP9 result, $B_0 < 3.37$, it improves the upper bound by a factor 3.7. Second, by adding lensing data the results can be further improved by a factor 5.1 ($B_0 < 0.18$). Finally, we arrive at our best bound of $B_0 < 0.12$ by using all data sets. In addition, we notice that, due to the degeneracy between B_0 and the dark matter density, the Planck data prefer a slightly lower value of $\Omega_c h^2$ in the $f(R)$ model. Consequently, this implies that $f(R)$ gravity favors a slightly larger value of H_0. This can be helpful to relax the tension between Planck and the other direct measurements of the Hubble parameter, such as that from the HST [87]. The degeneracy between B_0 and $\Omega_c h^2$ is illustrated in Fig. 7, where it

is evident that we can fit a lower value of the third peak by increasing B_0 while keeping $\Omega_c h^2$ fixed.

Marginalized likelihoods for all the parameters are shown in Fig. 3. We also highlight the 2D likelihood in the parameter space of B_0 and H_0 in Fig. 1 and the marginalized likelihood for B_0 in Fig. 2. Let us notice that the B_0 likelihood from WMAP9 data (gray curve) has a prominent second peak around $B_0 = 2.5$. This is due to the nonlinear dependence of the ISW effect on B_0 in $f(R)$ gravity. Since with WMAP resolution the lensing signal is quite weak, the main contribution to the B_0 constraint in WMAP data comes from the ISW effect. As shown in Fig. 6, under our parameter value choice (we fix all the other cosmological parameters as the mean values of the Planck base ΛCDM model), from $B_0 = 0$ to $B_0 \sim 1$ the slope of the spectrum in the ISW-dominated regime becomes gradually flat and approaches the Sachs-Wolfe plateau. After that, if it continues to increase until $B_0 \sim 2$, the power spectrum will bounce again and get closer to that of general relativity. If one further increases the B_0 value, the spectrum curve in the ISW regime will rise up above that of general relativity. Moreover, once we marginalize over all the other cosmological parameters, the turning point $B_0 \sim 1$ will shift to around $B_0 \sim 1.5$, and the second peak $B_0 \sim 2$ will move to $B_0 \sim 2.5$.

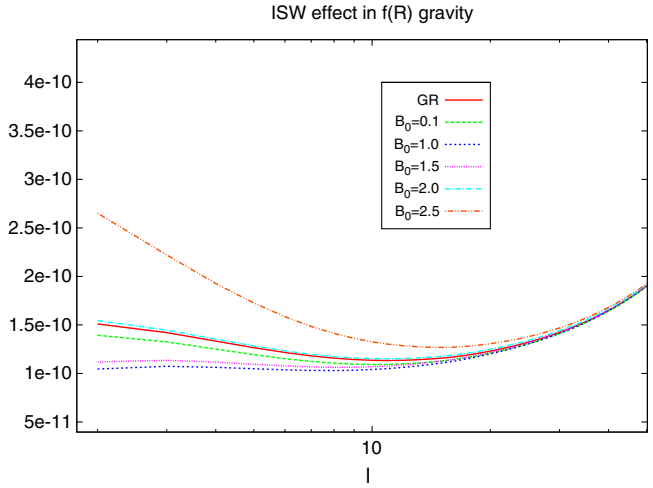

FIG. 6 (color online). The nonlinear dependence of the ISW effect on B_0 in $f(R)$ gravity.

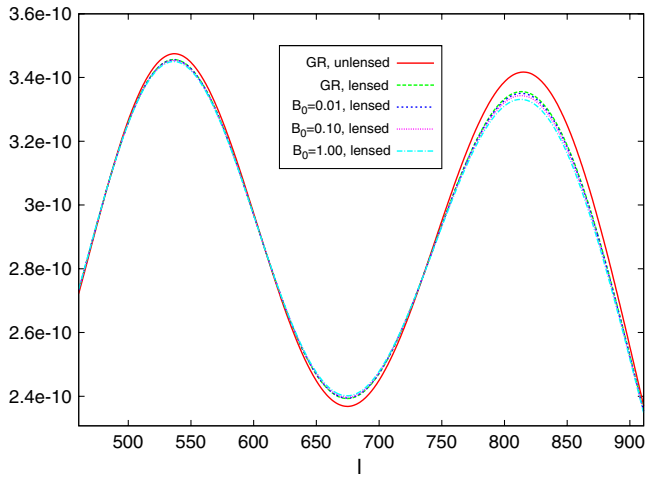

FIG. 7 (color online). The second and third peaks in $f(R)$ gravity. The larger B_0 is, the lower the third peak is.

Compared with $f(R)$ gravity, the chameleon-type model includes the other two free parameters β_1 and s, which are fixed to $4/3$ and 4 in the former case. Due to the amount of extra modified gravity parameters and the degeneracy among them, we find that the Planck constraints on the parameters B_0 and s are still quite loose, with no obvious improvement when comparing to WMAP9 results. However, we are able to improve the constraints on β_1: we find $\beta_1 = 1.043^{+0.163}_{-0.104}$ at 95% C.L. compared with $\beta_1 = 0.893^{+0.647}_{-0.695}$ at 95% C.L. from WMAP9. The detailed global analysis results can be found in Table III and Fig. 5. Confidence regions in the β_1-H_0 plane, after marginalizing over the other parameters, are shown in Fig. 4. One could notice that the value $\beta_1 = 4/3$, corresponding to $f(R)$ models, is well outside the 3σ confidence region. However, this does not rule out the $f(R)$ model by any means, given the very loose constraints on the other two relevant $f(R)$ parameters B_0 and s. In Fig. 8, we compare the likelihood of β_1 with(out) marginalization over B_0 by using Planck + WP + lensing + BAO + HST + Union 2 data sets. It clearly shows that the stringent constraint on β_1 is due to the marginalization effect on B_0, whose constraint is very loose for the chameleon-type model via current data sets. And we have also tested that if we fix $B_0 = 0.001$ and use the same data sets, the marginalized 2σ confidence level for β_1 is $0.971^{+0.700}_{-0.746}$, which reconciles with $f(R)$ gravity very well. We can also see in Table III that the

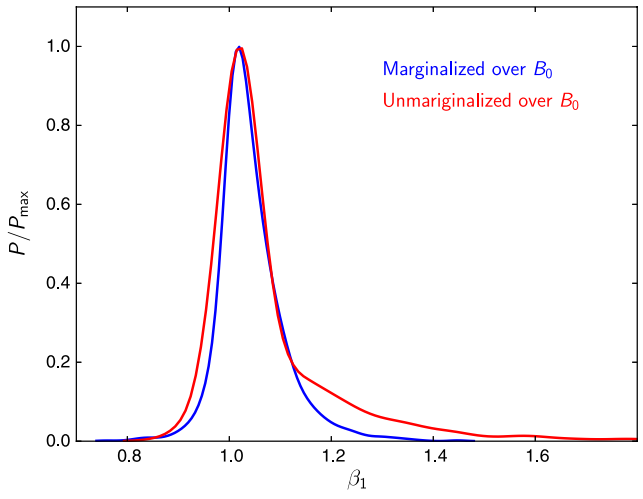

FIG. 8 (color online). Likelihood of β_1 with(out) marginalization over B_0 by using Planck + WP + Lensing + BAO + HST + Union 2 data sets.

chameleon-type model favors a slightly higher Hubble parameter, for the same reason as explained for $f(R)$ gravity.

ACKNOWLEDGMENTS

N. B. and B. H. are indebted to Philippe Brax for useful discussions. We also thank Jason Dossett, Alireza Hojjati, and Alessandra Silvestri for useful correspondence and discussion of the numerical codes. B. H. thanks Zhenhui Zhang for discussions and ITP-CAS for hospitality during the completion of some parts of this work. The numerical calculations are performed on clusters at ITP-CAS and INFN-PD. The research of N. B., M. L. and S. M. has been partially supported by the ASI/INAF Agreement No. I/072/09/0 for the Planck LFI Activity of Phase E2.

[1] E. Bertschinger, Astrophys. J. **648**, 797 (2006).
[2] Y.-S. Song, W. Hu, and I. Sawicki, Phys. Rev. D **75**, 044004 (2007).
[3] P. Brax, C. van de Bruck, A.-C. Davis, and D. J. Shaw, Phys. Rev. D **78**, 104021 (2008).
[4] G.-B. Zhao, L. Pogosian, A. Silvestri, and J. Zylberberg, Phys. Rev. Lett. **103**, 241301 (2009).
[5] G.-B. Zhao, T. Giannantonio, L. Pogosian, A. Silvestri, D. J. Bacon, K. Koyama, R. C. Nichol, and Y.-S. Song, Phys. Rev. D **81**, 103510 (2010).
[6] A. Hojjati, G.-B. Zhao, L. Pogosian, A. Silvestri, R. Crittenden, and K. Koyama, Phys. Rev. D **85**, 043508 (2012).
[7] E. Bertschinger and P. Zukin, Phys. Rev. D **78**, 024015 (2008).
[8] P. Brax, A.-C. Davis, B. Li, and H. A. Winther, Phys. Rev. D **86**, 044015 (2012).
[9] J. Zuntz, T. Baker, P. Ferreira, and C. Skordis, J. Cosmol. Astropart. Phys. 06 (2012) 032.
[10] A. Hojjati, L. Pogosian, A. Silvestri, and S. Talbot, Phys. Rev. D **86**, 123503 (2012).
[11] W. Hu and I. Sawicki, Phys. Rev. D **76**, 104043 (2007).
[12] W. Fang, W. Hu, and A. Lewis, Phys. Rev. D **78**, 087303 (2008).
[13] L. Lombriser, J. Yoo, and K. Koyama, Phys. Rev. D **87**, 104019 (2013).
[14] T. Baker, P. G. Ferreira, C. Skordis, and J. Zuntz, Phys. Rev. D **84**, 124018 (2011).
[15] T. Baker, P. G. Ferreira, and C. Skordis, Phys. Rev. D **87**, 024015 (2013).
[16] N. Arkani-Hamed, H.-C. Cheng, M. A. Luty, and S. Mukohyama, J. High Energy Phys. 05 (2004) 074.
[17] G. Gubitosi, F. Piazza, and F. Vernizzi, J. Cosmol. Astropart. Phys. 02 (2013) 032.
[18] J. K. Bloomfield, E. E. Flanagan, M. Park, and S. Watson, J. Cosmol. Astropart. Phys. 08 (2013) 010.
[19] P. Creminelli, M. A. Luty, A. Nicolis, and L. Senatore, J. High Energy Phys. 12 (2006) 080.
[20] C. Cheung, P. Creminelli, A. L. Fitzpatrick, J. Kaplan, and L. Senatore, J. High Energy Phys. 03 (2008) 014.
[21] P. Creminelli, G. D'Amico, J. Norena, and F. Vernizzi, J. Cosmol. Astropart. Phys. 02 (2009) 018.
[22] J. Gleyzes, D. Langlois, F. Piazza, and F. Vernizzi, J. Cosmol. Astropart. Phys. 08 (2013) 025.
[23] J. Bloomfield, arXiv:1304.6712.
[24] R. K. Sachs and A. M. Wolfe, Astrophys. J. **147**, 73 (1967); Gen. Relativ. Gravit. **39**, 1929 (2007).
[25] P. Zhang, Phys. Rev. D **73**, 123504 (2006).
[26] S. Ho, C. Hirata, N. Padmanabhan, U. Seljak, and N. Bahcall, Phys. Rev. D **78**, 043519 (2008).
[27] S. F. Daniel, E. V. Linder, T. L. Smith, R. R. Caldwell, A. Cooray, A. Leauthaud, and L. Lombriser, Phys. Rev. D **81**, 123508 (2010).
[28] A. Marchini, A. Melchiorri, V. Salvatelli, and L. Pagano, Phys. Rev. D **87**, 083527 (2013).
[29] R. Bean and M. Tangmatitham, Phys. Rev. D **81**, 083534 (2010).
[30] E. Di Valentino, A. Melchiorri, V. Salvatelli, and A. Silvestri, Phys. Rev. D **86**, 063517 (2012).
[31] B. Hu, M. Liguori, N. Bartolo, and S. Matarrese, Phys. Rev. D **88**, 024012 (2013).
[32] K. Yamamoto, B. A. Bassett, R. C. Nichol, and Y. Suto, Phys. Rev. D **74**, 063525 (2006).
[33] N. Said, C. Baccigalupi, M. Martinelli, A. Melchiorri, and A. Silvestri, Phys. Rev. D **88**, 043515 (2013).
[34] T. Giannantonio, M. Martinelli, A. Silvestri, and A. Melchiorri, J. Cosmol. Astropart. Phys. 04 (2010) 030.
[35] J. Dossett, J. Moldenhauer, and M. Ishak, Phys. Rev. D **84**, 023012 (2011).
[36] Y.-S. Song, H. Peiris, and W. Hu, Phys. Rev. D **76**, 063517 (2007).
[37] B. Jain and P. Zhang, Phys. Rev. D **78**, 063503 (2008).
[38] L. Lombriser, A. Slosar, U. Seljak, and W. Hu, Phys. Rev. D **85**, 124038 (2012).
[39] S. Ferraro, F. Schmidt, and W. Hu, Phys. Rev. D **83**, 063503 (2011).
[40] L. Lombriser, B. Li, K. Koyama, and G.-B. Zhao, Phys. Rev. D **87**, 123511 (2013).
[41] B. Li, W. A. Hellwing, K. Koyama, G.-B. Zhao, E. Jennings, and C. M. Baugh, Mon. Not. R. Astron. Soc. **428**, 743 (2013).
[42] S. Asaba, C. Hikage, K. Koyama, G.-B. Zhao, A. Hojjati, and L. Pogosian, J. Cosmol. Astropart. Phys. 08 (2013) 029.
[43] E. Jennings, C. M. Baugh, B. Li, G.-B. Zhao, and K. Koyama, Mon. Not. R. Astron. Soc. **425**, 2128 (2012).
[44] A. Raccanelli, D. Bertacca, D. Pietrobon, F. Schmidt, L. Samushia, N. Bartolo, O. Dore, S. Matarrese *et al.*, arXiv:1207.0500.
[45] S. A. Thomas, F. B. Abdalla, and J. Weller, Mon. Not. R. Astron. Soc. **395**, 197 (2009).
[46] Y.-C. Cai and G. Bernstein, Mon. Not. R. Astron. Soc. **422**, 1045 (2012).
[47] P. Zhang, M. Liguori, R. Bean, and S. Dodelson, Phys. Rev. Lett. **99**, 141302 (2007).

[48] C. M. Hirata, S. Ho, N. Padmanabhan, U. Seljak, and N. A. Bahcall, Phys. Rev. D **78**, 043520 (2008).
[49] G.-B. Zhao, L. Pogosian, A. Silvestri, and J. Zylberberg, Phys. Rev. D **79**, 083513 (2009).
[50] I. Laszlo, R. Bean, D. Kirk, and S. Bridle, arXiv:1109.4535.
[51] I. Tereno, E. Semboloni, and T. Schrabback, Astron. Astrophys. **530**, A68 (2011).
[52] R. Reyes, R. Mandelbaum, U. Seljak, T. Baldauf, J. E. Gunn, L. Lombriser, and R. E. Smith, Nature (London) **464**, 256 (2010).
[53] X. Wang, X. Chen, and C. Park, Astrophys. J. **747**, 48 (2012).
[54] A. Hall, C. Bonvin, and A. Challinor, Phys. Rev. D **87**, 064026 (2013).
[55] K. Yamamoto, G. Nakamura, G. Hutsi, T. Narikawa, and T. Sato, Phys. Rev. D **81**, 103517 (2010).
[56] J.-h. He, Phys. Rev. D **86**, 103505 (2012).
[57] H. Gil-Marin, F. Schmidt, W. Hu, R. Jimenez, and L. Verde, J. Cosmol. Astropart. Phys. 11 (2011) 019.
[58] N. Bartolo, E. Bellini, D. Bertacca, and S. Matarrese, J. Cosmol. Astropart. Phys. 03 (2013) 034.
[59] G.-B. Zhao, B. Li, and K. Koyama, Phys. Rev. D **83**, 044007 (2011).
[60] J.-h. He, B. Li, and Y. Jing, Phys. Rev. D **88**, 103507 (2013).
[61] B. Li, D. F. Mota, and J. D. Barrow, Astrophys. J. **728**, 109 (2011).
[62] P. A. R. Ade *et al.* (Planck Collaboration), arXiv:1303.5062.
[63] P. A. R. Ade *et al.* (Planck Collaboration), arXiv:1303.5075.
[64] P. A. R. Ade *et al.* (Planck Collaboration), arXiv:1303.5077.
[65] P. A. R. Ade *et al.* (Planck Collaboration), arXiv:1303.5084.
[66] P. A. R. Ade *et al.* (Planck Collaboration), arXiv:1303.5079.
[67] Y.-C. Li, F.-Q. Wu, and X. Chen, Phys. Rev. D **88**, 084053 (2013).
[68] M. Li, X.-D. Li, Y.-Z. Ma, X. Zhang, and Z. Zhang, J. Cosmol. Astropart. Phys. 09 (2013) 021.
[69] V. Pettorino, Phys. Rev. D **88**, 063519 (2013).
[70] V. Salvatelli and A. Marchini, Phys. Rev. D **88**, 023531 (2013).
[71] A. Marchini and V. Salvatelli, Phys. Rev. D **88**, 027502 (2013).
[72] J.-h. He, arXiv:1307.4876.
[73] D. F. Mota and D. J. Shaw, Phys. Rev. D **75**, 063501 (2007).
[74] P. Brax, C. van de Bruck, A.-C. Davis, J. Khoury, and A. Weltman, Phys. Rev. D **70**, 123518 (2004).
[75] M. Pietroni, Phys. Rev. D **72**, 043535 (2005).
[76] K. A. Olive and M. Pospelov, Phys. Rev. D **77**, 043524 (2008).
[77] K. Hinterbichler and J. Khoury, Phys. Rev. Lett. **104**, 231301 (2010).
[78] P. Brax, C. van de Bruck, A.-C. Davis, and D. Shaw, Phys. Rev. D **82**, 063519 (2010).
[79] A. Hojjati, L. Pogosian, and G.-B. Zhao, J. Cosmol. Astropart. Phys. 08 (2011) 005.
[80] A. Lewis, A. Challinor, and A. Lasenby, Astrophys. J. **538**, 473 (2000).
[81] C. L. Bennett, D. Larson, J. L. Weiland, N. Jarosik, G. Hinshaw, N. Odegard, K. M. Smith, R. S. Hill *et al.*, Astrophys. J. Suppl. Ser. **208**, 20 (2013).
[82] G. Hinshaw *et al.* (WMAP Collaboration), Astrophys. J. Suppl. Ser. **208**, 19 (2013).
[83] A. De Felice and S. Tsujikawa, Living Rev. Relativity **13**, 3 (2010).
[84] F. Beutler, C. Blake, M. Colless, D. H. Jones, L. Staveley-Smith, L. Campbell, Q. Parker, W. Saunders, and F. Watson, Mon. Not. R. Astron. Soc. **416**, 3017 (2011).
[85] W. J. Percival *et al.* (SDSS Collaboration), Mon. Not. R. Astron. Soc. **401**, 2148 (2010).
[86] L. Anderson, E. Aubourg, S. Bailey, D. Bizyaev, M. Blanton, A. S. Bolton, J. Brinkmann, J. R. Brownstein *et al.*, Mon. Not. R. Astron. Soc. **427**, 3435 (2013).
[87] W. L. Freedman *et al.* (HST Collaboration), Astrophys. J. **553**, 47 (2001).
[88] N. Suzuki, D. Rubin, C. Lidman, G. Aldering, R. Amanullah, K. Barbary, L. F. Barrientos, J. Botyanszki *et al.*, Astrophys. J. **746**, 85 (2012).
[89] N. Padmanabhan, X. Xu, D. J. Eisenstein, R. Scalzo, A. J. Cuesta, K. T. Mehta, and E. Kazin, Mon. Not. R. Astron. Soc. **427**, 2132 (2012).
[90] A. G. Riess, L. Macri, S. Casertano, H. Lampeitl, H. C. Ferguson, A. V. Filippenko, S. W. Jha, W. Li, and R. Chornock, Astrophys. J. **730**, 119 (2011); A. G. Riess, L. Macri, S. Casertano, H. Lampeit, H. C. Ferguson, A. V. Filippenko, S. W. Jha, W. Li, R. Chornock, and J. M. Silverman, Astrophys. J. **732**, 129(E) (2011).
[91] A. Lewis and S. Bridle, Phys. Rev. D **66**, 103511 (2002).
[92] P. A. R. Ade *et al.* (Planck Collaboration), arXiv:1303.5076.